Available online at www.sciencedirect.com
ScienceDirect
Journal of Environmental Sciences 19(2007) 948–954
JOURNAL OF ENVIRONMENTAL SCIENCES
ISSN 1001-0742
CN 11-2629/X
www.jesc.ac.cn

Interaction of DNA with aromatic hydrocarbons fraction in atmospheric particulates of Xigu District of Lanzhou, China

GAO Hong[1,*], MA Min-quan[2], ZHOU Lei[3], JIA Run-ping[3], CHEN Xing-guo[3], HU Zhi-de[3]

1. Key Laboratory of Western China's Environmental Systems (Ministry of Education), College of Earth and Environment Sciences, Lanzhou University, Lanzhou 730000, China. E-mail: honggao@lzu.edu.cn
2. Lanzhou Environmental Monitoring Station, Lanzhou 730000, China
3. Department of Chemistry, Lanzhou University, Lanzhou 730000, China

Received 7 September 2006; revised 11 December 2006; accepted 19 March 2007

Abstract

Voluminously epidemiological studies show that the relationships exist between the air pollution and human health and cancer. Aromatic hydrocarbons (AHs) in air form a large class of organic pollutants, which are widely in environment and many of them are known to be carcinogenic and/or mutagenic and contribute to ambient air pollution. In the past decades, bioassays mainly have been used to evaluate the toxicity of chemical mixtures in atmospheric particulates or aqueous environment. However, it is well known that the covalent complexes formed by carcinogens with DNA may be exert negative results in bioassay. So the main aim of this paper is to develop an evaluation method of toxicity effects of chemical mixtures in atmospheric particulates from chemical standpoint. In this study, the *in vitro* interaction of the AHs with DNA was investigated by absorption, fluorescence and resonance light scattering (RLS) spectroscopic techniques. The results showed that the AHs in the atmospheric particulates could combine with calf thymus DNA (ctDNA) and herring sperm DNA (hsDNA) without being activated or metabolized by organism, respectively. Intercalation may be present in the mechanism of interaction. The binding constants of the AHs with ctDNA and hsDNA were 2.5×10^2 and 2.0×10^3, respectively, which indicated that the interaction of the AHs with hsDNA is stronger than that with ctDNA. In addition, the relationships of dose-effect between the total mole concentration of chemical components and the ability of binding ctDNA and hsDNA were confirmed. This research made it possible to study the toxicity effects of chemical mixtures in atmospheric particulates by chemical method. It is believed that the composition and contents of unknown AHs and the interaction of DNA with AHs in atmospheric particulates of Xigu District of Lanzhou City, China are first reported in the past twenty years.

Key words: atmospheric particulates; aromatic hydrocarbons fraction; interaction with DNA

Introduction

In recent years, with the rapid development of industry and agriculture, more and more attention has been paid to the problems of human exposure to man-made chemicals because a larger number of chemical substances have been released into environment and caused serious health problems (Bert and Stephen, 2002). Since 1970s, there has be increasing evidence that environmental chemicals play an important role in the causation of cancer (Hiatt *et al*., 1977). Furthermore, many epidemiological studies have shown a significant association between exposure to airborne particulate matters and daily morbidity and mortality (Schwartz, 2000; Dockery, 2001; Pope, 1996). In addition, other numbers of analytical studies have also shown that a lot of mutagenic and carcinogenic substances including organic compounds and inorganic compounds have been adsorbed on particulates in urban air (Sicre *et al*., 1987; Sun *et al*., 2003; IARC, 1990, 1994). Among them, aromatic hydrocarbons (AHs), especially polycyclic aromatic hydrocarbons (PAHs) are widely distributed in particles and in vapour phase and form a large class of organic compounds; many of these AHs or PAHs are mutagenic and carcinogenic, therefore, they may have a potential health impact on human beings (Martel *et al*., 1986).

During the past decades, a widely variety of bio-test systems have been developed for the toxicity testing of exposure to chemicals such as the Ames assay for monitoring the mutagenic potential of complex environmental mixtures, *in vitro* micronucleus assay for chromosomal alterations, comet assay for primary DNA damage, transgenic animals for detection of gene mutations *in vivo*, and fluorescent *in situ* hybridization method for detection of aneuploidy (Ames *et al*., 1975; Marzin, 1999). Namely, the biological effects of mutagen and carcinogen on human body or other living organism exert mainly through mechanism involving the DNA damage (Wu *et al*., 2002). However, according to literature reports that a large number of well-known carcinogens are formed

Project supported by the Excellent Doctor Foundation of Lanzhou University. *Corresponding author. E-mail: honggao@lzu.edu.cn.

covalent complexes with DNA (Kyrtopoulos *et al*., 1997). So some of carcinogens may be obtained negative results in Ames *et al*. (1975) bio-test assay. As a matter of fact, complex chemical component exert a synthetically toxicological effect on human bodies due to that humans are exposed to differing of complex chemical mixtures from their atmospheric environment. So it is important to investigate the complex chemical component and the relationships between component concentration and toxicological effect. Yet it is difficult to study the correlation between the analyzing data of chemical mixtures and genotoxicity results. Previous studies have mainly focused on analyzing chemical composition or evaluating the potential genotoxic risk of such mixtures and usually established an oversimplified relationship of dose-effect between the total contents of chemical extracts and genotoxicity results by bio-test. The aim of this study is not only to investigate the interaction of a class of AHs with DNA but also to establish a method to evaluate the relationships of dose-effect between the total contents of AHs and genotoxicity results from chemical standpoint.

Lanzhou is the capital city of Gansu Province and located in northwest of China, Xigu District of Lanzhou City is an important petrochemical industrial base and also the first place that photochemical smog occurs in China. Large quantities of industrial, traffic and domestic exhaust gas as well as its special geographical position and topographical conditions make it as one of the most serious air polluted cities in the world (Zhang *et al*., 2000). So it is very significant to investigate constitutes and concentrations of aromatic hydrocarbons in atmospheric particulates and the correlation between chemical mixtures content and genotoxicity result.

Fluorescence and absorption spectrometry are being widely used to study the binding between small molecules and biomacromolecules (Aich *et al*., 1992; Scatchard *et al*., 1950; Plsavento and Porfumo, 1991; Gupta and Ali, 1984). In recent years, these techniques have been also applied in the field of Chinese traditional herbal medicine, for example, the interaction of active components in Chinese traditional herbal medicine with biomacromolecules such as bovine serum albumins has been well studied in detail using these techniques (Liu *et al*., 2003; Tian *et al*., 2003). But the tentative application of these techniques is uncommonly reported in the field of environmental science, Guo *et al*. (2000) studied the binding reaction of PAHs part in Taiyuan City floating dust with DNA using the method fluorescence method. In addition, there is an another technique, resonance light scattering (RLS), also used to study the binding between small molecules and biomacromolecules recently (Huang *et al*., 2001; Zhang *et al*., 2001). The enhanced RLS signals, which are originally discovered from the binding of dye to biomacromolecules, are mainly applied to the determination of nucleic acids or proteins in biological samples because a good linear relationship could be established between target compound concentration and the enhanced RLS signals (Pasternack and Collings, 1995). In this article, the application of absorption, fluorescence and RLS spectrometry for studying the interaction of DNA with the complex AHs in atmospheric particulates *in vitro* was reported. And a good linear-relationship of dose-effect between the total contents of chemical mixtures of AHs and the ability of binding DNA was observed.

1 Materials and methods

1.1 Reagent and chemicals

Dichloromethane, hexane, benzene and dimethyl sulphoxide from The Second Tianjin Chemical Reagent Factory (Tianjin, China) were of analytical grade and were redistilled prior to use. Commercially prepared calf thymus DNA (ctDNA) and herring sperm DNA (hsDNA), obtained from Huamei Chemical Company (China), were dissolved in 0.05 mol/L Tris-HCl buffer solution (pH 7.4) as stock solution and stored at 4°C. The stock solutions were further diluted as working solutions prior to use. The ratio of absorptions of ctDNA and hsDNA at 260 nm/280 nm are 1.9 and 1.8, respectively, indicating that the DNA was sufficiently free of protein. The accurate concentrations of ctDNA and hsDNA were determined by UV absorbance at 260 nm in dilutions. The extinction coefficient ε_{260} was taken as 6600 mol^{-1} cm^{-1} (Tysoe *et al*., 1993). A buffer solution of pH 7.4 was prepared by weighing 3.0285 g Tris and 212.5 ml of 0.1 mol/L HCl and adding water to a final volume of 500 ml. Water used throughout was doubly distilled.

1.2 Sampling of atmospheric particulates

A high-volume air sampler (TH-1000C, Tianhong Intelligent Instrument Plant of Wuhan, China) fitted with glass fiber filter (20 cm × 25 cm) was used to collected atmospheric particulate matter at a flow rate of 0.8 m^3/min. In March 2003, six samples were obtained from the Lanyuan Hotel of Xigu District in Lanzhou City (National Control Monitoring Site) and each sample was collected during a 24-h periods.

1.3 Extraction and isolation of aromatic fraction from TSP

The total suspended particulate matter (TSP) in the glass fiber filters was firstly extracted using an ultrasonic bath with dichloromethane. Subsequently, the extract was concentrated by a Bchi rotary evaporator (bath temperature <30°C) and isolated by silica gel column chromatography with 130 ml hexane (for the aliphatic hydrocarbons fraction) and 400 ml benzene (for the AHs fraction) as elute solvents. Then the benzene elute was concentrated to volumes of approximately 3 ml by the rotary evaporator and transferred to a glass vial which was weighed prior to use. Finally the benzene elute in the glass vial was volatilizeded to dryness under a gentle stream of ultra pure nitrogen and weighed again. The difference of twice weighing between the glass vial and the glass vial with the dryness elute was the extract yields of the AHs fraction separated. Then the benzene elute was redissolved with 100 μl benzene for GC-MS and GC analysis.

1.4 Analysis of chemical components of aromatic fraction

Qualitative analysis was tentatively identified by GC-MS (TRACE GC-MS™, Finnigan, USA) equipped with a SE-54 fused-silica capillary column (30 m × 0.25 mm i.d., 0.25 μm film thickness). The following temperature program was used: the initial column temperature was 50°C and programmed at 8°C/min to 150°C, then at 3°C/min to 280°C held for 5 min. A split/splitless injector and the detector temperatures were set at 280°C and 300°C, respectively. Helium was the carrier gas at a flow-rate of 1.0 ml/min. 1.0 μl sample extracts was injected in split mode at a ratio of 20:1. The electron impact (EI) ionization conditions were: ion energy 70 eV and mass range (*m/z*) 15.00–431.00 in the full scan mode.

The aromatic fraction was quantified by GC with FID (VarianCP-3800, USA) equipped with the same type of column as that used for the GC-MS analysis. Nitrogen as a carrier gas at a flow rate of 1.4 ml/L and 1.0 μl sample extracts was injected in split mode at a ratio of 20:1. A split/splitless injector and the detector were maintained at 280°C and 300°C, respectively. The column temperature program began with 50°C followed by a 8°C/min ramp to 150°C and then a 3°C/min ramp to 280°C held for 30 min. A novel calculation method with the FID relative carbon weight response factors of hydrocarbons for FID quantitative analysis was used in order to resolve the lack of standards (Huang *et al*., 1990; You *et al*., 1999).

1.5 Interaction studies of DNA with aromatic fraction

The benzene elute after GC-MS and GC analysis was volatilizeded to dryness under a gentle stream of ultra pure nitrogen and then redissolved with dimethyl sulphoxide (DMSO). That the DMSO solution dissolved benzene elute would be abridged as AHs-DMSO in the following part of paper. The AHs-DMSO solution was stored at 4°C for a series of spectral studies.

Two sets of the reaction mixture solutions were prepared with AHs-DMSO and ctDNA or hsDNA. Transferred 0.2 ml of AHs-DMSO solution (1.7×10^{-3} mol/L) to a 10-ml standard volumetric flask with a stopper. Added a set of known volume of ctDNA or hsDNA (the concentrations were 2.8×10^{-3} and 2.5×10^{-3} mol/L, respectively) standard solution. Diluted to volume with buffer and mixed. Both the mixed solution and a reagent blank (prepared in a similar manner without AHs or DNA) were allowed to incubate at 25°C for 48 h. Scanned the absorption, fluorescence, and RLS spectra, and recorded the intensities of fluorescence and RLS spectra.

Absorption spectra were scanned with a Shimadzu UV-240 ultraviolet-visible spectrophotometer in the wavelength range of 190–400 nm, using 1.0 cm quartz cells. All fluorescence and RLS measurements were made using a Shimadzu RF-5301PC spectrofluorimeter equipped with a xenon lamp source and 1.0 cm quartz cells. For fluorescence spectra, the excitation and emission wavelengths were 334 and 391 nm, respectively, and the excitation and emission bandwidths were both 5 nm. For RLS spectra, the excitation wavelengths (equal to emission wavelengths) was 402 nm and the excitation bandwidths (equal to emission bandwidths) was 1.5 nm.

2 Results and discussion

2.1 Chemical components in AHs

More than one hundred and forty benzene derivatives and PAHs were discovered in AHs fraction (Table 1 and Fig.1). In benzene derivatives class, there were some substituted benzene compounds by alkyl, chloro, bromo, nitro and amino, few substituted phenols and contain-

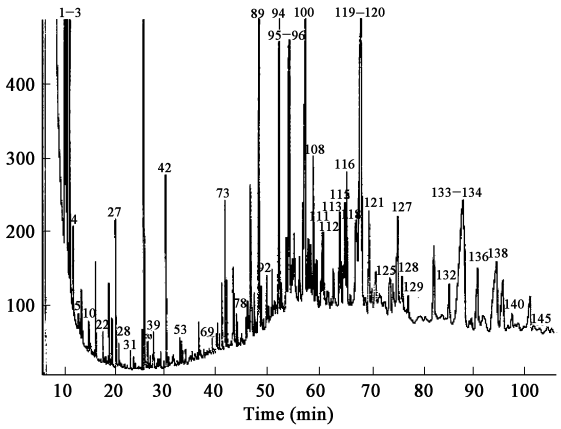

Fig. 1 Gas chromatogram of the aromatic hydrocarbons fraction in the TSP.

Table 1 Peak number, name and content of aromatic pollutants in the TSP

No.	Compound	Content (ng/m^3)	No.	Compound	Content (ng/m^3)
1	Chlorobenzene*	988	14	4-Ethoxy-benzoic acid ethyl ester	0.43
2	Ethylbenzene*	202	15	Dibenzofuran	1.95
3	α-Methylbenzeneacetaldehyde	314	16	1-Methyl-2,4-dinitrobenzene	3.34
4	1-Methylethylbenzene	18.2	17	iso-Trimethylnaphthalene	1.27
5	Bromobenzene	5.74	18	*iso*-Trimethylnaphthalene	0.79
6	Propylbenzene	3.0	19	*iso*-Trimethylnaphthalene	1.33
7	1,3,5-Trimethylbenzene	0.35	20	*iso*-Chlorobiphenyl	1.53
8	1,4-Dichlorobenzene*	1.63	21	*iso*-Chlorobiphenyl	11.3
9	1-Ethyl-3-methylbenzene	0.61	22	1H-Phenalene	8.07
10	1-Chloro-2-ethylbenzene	9.50	23	2,2'-Dimethylbiphenyl	0.81
11	1-Chloro-4-ethylbenzene	0.61	24	1-Methyl-7-(1-methylethyl) naphthalene	7.45
12	1,4-Diethylbenzene	0.66			
13	*trans*-Decahydronaphthalene	0.11	25	4-Methyldibenzofuran	2.71

Table 1 continued

No.	Compound	Content (ng/m^3)	No.	Compound	Content (ng/m^3)
26	1-Methyl-2-propylbenzene	0.10	83	Benzophenone	4.29
27	Acetophenone	0.95	84	9H-Xanthene	0.96
28	*iso*-Dimethyl-*iso*-ethylbenzene	0.37	85	3,4-Diethyl-1,1'-biphenyl	0.18
29	1-Methyl-4-(1-methylethyl) benzene	1.29	86	9,9-Dimethyl-9-silafluorene	1.01
			87	*iso*-Methyl-9H-fluorene	2.61
30	*iso*-Dimethyl-*iso*-ethylbenzene	1.48	88	*iso*-Methyl-9H-fluorene	0.95
31	Nitrobenzene*	0.19	89	2,6-Diisopropylnaphthalene	5.41
32	1,2,4,5-Tetramethylbenzene	0.42	90	1,6-Dimethyl-4-(1-methylethyl) naphthalene	1.19
33	*iso*-Dimethyl-*iso*-ethylbenzene	0.78			
34	2-Nitrophenol*	15.5	91	2-(phenylmethylene)octanal	0.49
35	1-Methyl-4-(1-methylethenyl) benzene	0.11	92	9H-Fluoren-9-one	0.64
			93	3,5-Di-tert-butyl-4-hydroxybenzaldehyde	1.04
36	1-Methyl-4-(1-methylpropyl) benzene	0.46			
			94	Dibenzothiophene	9.08
37	1,2,3,4-Tetrahydronaphthalene	1.10	95	Benzylbenzoate	1.39
38	Ethylbenzoate	1.03	96	9-Methylene-9H-fluorene	7.85
39	4-Bromobenzenamine	109	97	Phenanthrene*	8.47
40	Benzothiazole	14.9	98	Anthracene*	0.58
41	4-Methyl-2-nitrophenol	2.05	99	Bis(2-methylpropyl) phthalate	95.6
42	1,5-Dimethyl-1,2,3,4-tetrahydronaphthalene	0.22	100	(Phenoxymethyl)-benzene	31.9
			101	Thioxanthene	0.48
43	*iso*-Dimethylnaphthalene	5.77	102	4b,8-Dimethyl-2-isopropyl-4b,5,6,7,8,8a,9,10-octahydro phenanthrene	2.59
44	1-Ethylidene -1H-indene	4.58			
45	Benzenebutanenitrile	1.64			
46	2,6-Dimethyl-4-nitrophenol	1.12	103	*iso*-Methylphenanthrene	0.15
47	Diphenylether	9.24	104	*iso*-Methylphenanthrene	11.9
48	*iso*-Dimethyl-naphthalene	6.66	105	*iso*-Methylanthracene	0.64
49	*p*-Nitroaniline	1.92	106	6H-Cyclobuta[jk]phenanthrene	0.91
50	*iso*-Dimethyl-naphthalene	2.09	107	*iso*-Methylphenanthrene	1.96
51	2,6-Bis(1,1-dimethylethyl) phenol	9.70	108	*iso*-Methylphenanthrene	3.29
			109	Dibutyl phthalate*	2.36
52	Diphenylmethane	0.59	110	*iso*-Methylcarbazole	1.01
53	*iso*-Dimethylnaphthalene	3.80	111	*iso*-Methylcarbazole	9.83
54	Butylated hydroxytoluene	127	112	9,10-Di(chloromethyl) anthracene	21.3
55	*iso*-Chlorobiphenyl	4.49			
56	2-(1-Methylethyl)naphthalene	0.79	113	9,10-Anthracenedione	6.61
57	2-Mercaptobenzothiazole	31.3	114	Triphenylene	16.9
58	3.3'-Diphenyl-5-methyl -3H-pyrazole	258	115	Benz[c]acridine	52.3
			116	Benz[a]anthracene-7,12-dione	73.2
59	3,7-Dimethylphenothiazine	27.1	117	Benzo[b]naphtho[2,3-d]thiophene	6.93
60	Oxybenzone	8.15	118	Benz[a]anthracene*	121
61	2-Ethylanthracene	19.7	119	Chrysene*	538
62	2,7-Dimethylphenanthrene	21.3	120	Benzo[b]carbazole	180
63	Fluoranthene*	245	121	6-Methyl-benzo[b]naphtho [2,4-d]thiophene	89.3
64	Pyrene*	252			
65	Benzo[b]naphtho[2,3-d]furan	12.9	122	Di-*n*-octyl phthalate	16.9
66	2-Propenoic acid, 3-[4-methoxyphenyl]-2-ethylhexyl ester	2.00	123	7H-Benzo[c]carbazole	9.82
			124	11H-Benzo[a]carbazole	0.58
			125	1-Nitrofluoranthene	72.5
67	1-Hydroxypyrene	2.11	126	11-Methylbenz[a]anthracene	17.5
68	Benzo[b]naphtho[2,1-d]furan	45.6	127	*iso*-Methtylchrysene	108
69	9-Butyl-1,2,3,4-tetrahydro -anthracene	52.2	128	*iso*-Dimethylbenz[a]anthracene	35.5
			129	2,2'-Binaphthalene	19.5
70	Benzo[k]xanthene	9.37	130	9-Phenylanthracene	0.41
71	7H-Benzo[c]fluorene	12.7	131	*iso*-Dimethylbenz[a]anthracene	0.27
72	2,4,5,7-Tetramethylphenanthrene	0.25	132	1,2-Dihydroindeno[1,2,3-cd]pyrene	44.8
73	*iso*-Methylfluoranthene	42.5	133	Perylene	203
73	*n*-Phenyl-2-naphthalenamine	21.3	134	Benzo[e]pyrene	162
75	*iso*-Methypyrene	370	135	4,5-Oxide-benzo[a]pyrene	121
76	*iso*-Methylfluoranthene	38.4	136	1-Phenyl-naphtho[2,1-b]thiophene	90.4
77	1,4-Dimethyl-6-phenyl naphthalene	84.6	137	Benzo[k/j]fluoranthene*	1.03
			138	Benzo[a]pyrene*	236
78	1-Phenanthrenecarboxylic acid,1,2,3,4,4a, 9,10,10a-octahydro-1,4a-dimethyl-7-(1-methylethyl)-methyl ester	28.8	139	11H-Indeno[2,1-a]phenanthrene	0.15
			140	*iso*-Methylperylene	18.8
			141	3-Methylbenz[j]aceanthrylene	0.39
			142	3-Methyl-1-cholanthrenol	0.78
79	*o*-Terphenyl	12.4	143	*iso*-Methylperylene	0.19
80	1,3-Dimethylpyrene	30.1	144	3-Phenyl-(1H)phenanthro [9,10-d]pyrazole	0.60
81	7H-Benz[de]anthracen-7-one	29.9			
82	Benzo[b]naphtho[2,1-d]thiophene	71.6	145	Benzo[a]naphthacene	0.26

*. EPA priority pollutants were determined.

ing nitrogen, sulfur and oxygen heterocyclic compounds. While in PAHs class, most components with three to five rings were parent PAHs and alkyl substituted PAHs. Some were PAHs derivatives with two rings, polycyclic aromatic ketones and heterocyclic compoundscontaining nitrogen, sulfur and oxygen. In addition, few chloro and hydroxy substituted PAHs also existed in the fraction. Table 1 gave their peak number, name and content (ng/m^3) of aromatic pollutants in the TSP, in which 14 EPA priority pollutants were determined (by * marked). The benzo[a]pyrene (236 ng/m^3) exceeded the Ambient Air Quality Standard of China (10 ng/m^3) about 20 times. The total concentration of AHs-DMSO in moles per liter was calculated according to following equation: $[AHs]_t=\sum W_i/M_i$ (i=1–145, Table1), in which $[AHs]_t$ is the total mole concentration of AHs dissolved DMSO, W_i and M_i are the mass and the molecular weight of i component respectively.

2.2 Absorption studies

The change of absorption and fluorescence spectra after the binding between small molecules and biomacromolecules usually is used in the study of the interaction and their interaction mechanism. In order to confirm if the interaction could occur between DNA with AHs, the absorption and fluorescence spectra of free DNA or AHs and mixture of them were studied.

Figs.2 and 3 illustrate the absorption spectra of AHs, DNA and a change of the absorption spectra after mixing AHs with DNA, respectively. In Fig.2, the two bands were observed in the ultraviolet region and the intensity of the maximum of the peak at 213 nm and 264 nm respectively in ctDNA. The free AHs have an absorption peak at 226 nm. When ctDNA was added, the peak (226 nm) of AHs (ctDNA:0) red shift to 235 nm (ctDNA: 7.0×10^{-4} mol/L). Up to 1.4×10^{-3} mol/L of ctDNA concentration caused a coalition kurtosis, namely, broadening of the peaks. The further addition of ctDNA did not occur any additional changes in coalition kurtosis, this is considered for the saturation of binding of the AHs to the ctDNA. The spectra of hsDNA and the spectra changes of the mixture of AHs and hsDNA in Fig.3 showed similar characteristic with Fig.2. It is different that two absorption peaks of hsDNA at the wavelengths of 217 nm and 260 nm, respectively. With the increasing of the concentration of hsDNA, the free AHs peak red shift from 226 nm to 232 nm (hsDNA: 5.0×10^{-4} mol/L). When the mole concentration reached 1.0×10^{-3} mol/L, the coalition kurtosis formed. Continued addition of hsDNA did not occur any changes in coalition kurtosis spectra.

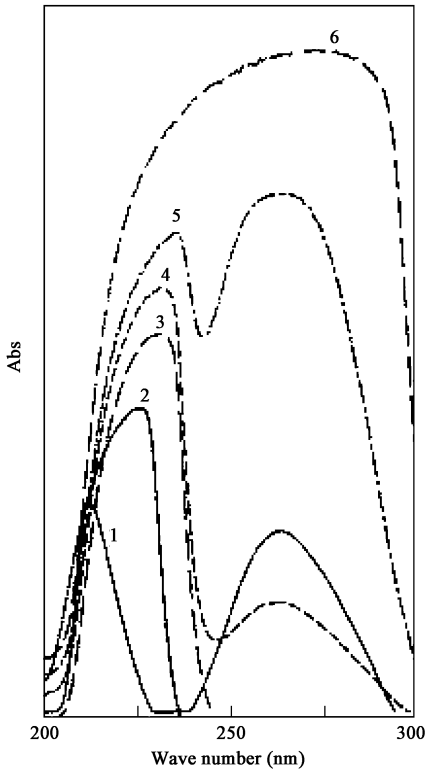

Fig. 2 Absorption spectra of the interaction of ctDNA with AHs. (1) ctDNA (2.8 × 10^{-4} mol/L); (2) AHs (3.3 × 10^{-5} mol/L); (3): ctDNA (1.4 × 10^{-4} mol/L) + AHs (3.3 × 10^{-5} mol/L); (4) ctDNA (2.8 × 10^{-4} mol/L) + AHs (3.3 × 10^{-5} mol/L); (5) ctDNA (7.0 × 10^{-4} mol/L) + AHs (3.3 × 10^{-5} mol/L); (6) ctDNA (1.4 × 10^{-3} mol/L) + AHs (3.3 × 10^{-5} mol/L).

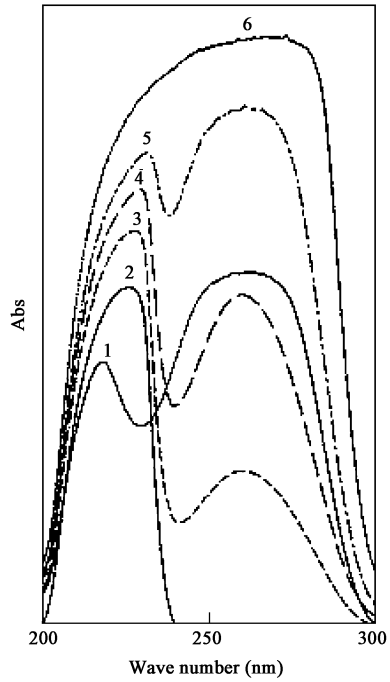

Fig. 3 Absorption spectra of the interaction of hsDNA with AHs. (1) hsDNA (2.5 × 10^{-4} mol/L); (2) AHs (3.3 × 10^{-5} mol/L); (3): hsDNA (1.25 × 10^{-4} mol/L) + AHs (3.3 × 10^{-5} mol/L); (4) hsDNA (2.5 × 10^{-4} mol/L) + AHs (3.3 × 10^{-5} mol/L); (5) hsDNA (5.0 × 10^{-4} mol/L) + AHs (3.3 × 10^{-5} mol/L); (6) hsDNA (1.0 × 10^{-3} mol/L) + AHs (3.3 × 10^{-5} mol/L).

That these pronounced changes including red-shifting and broadening of the peaks in the absorption spectra of AHs after mixing with different concentrations of ctDNA and hsDNA verified that the AHs fraction can bind to ctDNA and hsDNA (Aich *et al*., 1992).

2.3 Fluorescence studies

Fluorescence spectroscopy was used to further investigate the binding of AHs with ctDNA and hsDNA. Fig.4 and Fig.5 show the excitation and emission spectra of the

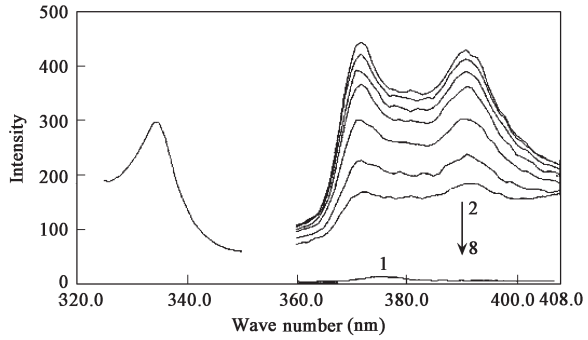

Fig. 4 Fluorescence excitation (left) and emission (right) spectra of the ctDNA-AHs system. (1) ctDNA (1.4×10^{-4} mol/L); (2) AHs (3.3×10^{-5} mol/L); (3–8): ctDNA (1.4×10^{-4}, 2.1×10^{-4}, 2.8×10^{-4}, 7.0×10^{-4}, 14.0×10^{-4}, 28.0×10^{-4} mol/L) + AHs (3.3×10^{-5} mol/L), respectively.

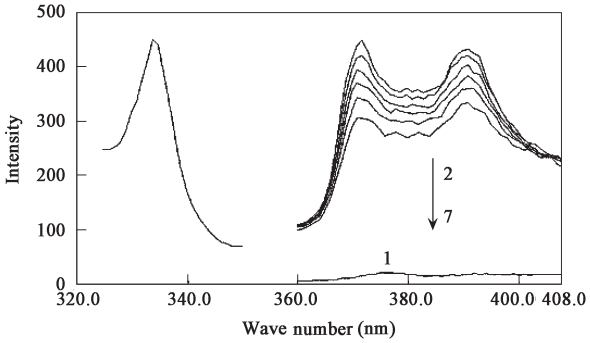

Fig. 5 Fluorescence excitation (left) and emission (right) spectra of the hsDNA-AHs system. (1) hsDNA (2.5×10^{-4} mol/L); (2) AHs (3.3×10^{-5} mol/L); (3–7) hsDNA (1.25×10^{-4}; 2.5×10^{-4}; 7.5×10^{-4}; 15.0×10^{-4}, 20.0×10^{-4} mol/L) + AHs (3.3×10^{-5} mol/L), respectively.

AHs-ctDNA and AHs-hsDNA system in the presence of various concentrations ctDNA or hsDNA. From the two figures, it can be seen that both ctDNA and hsDNA showed very little fluorescence intensities, but AHs fraction has strong fluorescence intensity. The excitation peak of AHs fraction was at 334 nm and two emission bands located at 372 and 391 nm respectively. The fluorescence intensity of AHs fraction was decreased regularly with the increasing of ctDNA or hsDNA concentration, indicating that a AHs-DNA complex, which could quench the fluorescence of AHs was formed, but the emission maximum at 372 and 391 nm remained unchanged. The results of fluorescence studies further supported the interaction of AHs fraction with ctDNA and hsDNA. Therefore, the above data are used to evaluate the binding constants (K) according to the equation (Lakowica, 1999):

$$C_{\mathrm{AHs}}/(F_0-F) = (kQ_{\mathrm{AD}})^{-1} + ((KkQ_{\mathrm{AD}})^{-1}(C_{\mathrm{DNA}})^{-1}) = A + B(C_{\mathrm{DNA}})^{-1} \quad (1)$$

Where, C_{AHs} is the fixed concentration of AHs and C_{DNA} is the concentration of DNA. F_0 and F are the fluorescence intensities in the absence and presence of DNA, respectively; K is the binding constant of DNA with AHs and k is a constant characteristic of the fluorophore and instrumental parameters, Q_{AD} is the quantum yield for the complex. A plot of $C_{\mathrm{AHs}}/(F_0-F)$ vs. $1/C_{\mathrm{DNA}}$ yields K ($K = A/B$). The binding constants of the AHs with ctDNA and hsDNA were 2.5×10^2 and 2.0×10^3, respectively, which indicated that the interaction of the AHs with hsDNA is stronger than that with ctDNA.

From the results of fluorescence studies, we could infer that the binding took place between AHs fraction and DNA (Aich *et al*., 1992) and the binding mechanism involved maybe is that some active components of AHs in the TSP intercalated the DNA bases (Gupta and Ali, 1984).

2.4 RLS studies

RLS spectra studies not only provides a binding support between small molecules and biomacromolecules but also can usually establish a well linear relationship between enhanced RLS signals of binding complex and the concentrations of fluorescent molecule. From this standpoint we tried to confirm the binding of AHs with DNA and establish a relationship between the total mole concentration of AHs and the RLS intensities of binding complex.

The RLS spectra of AHs, ctDNA (or hsDNA) and the mixture of AHs with ctDNA (or hsDNA) are shown in Fig.6 and Fig.7. It can be seen that all of AHs, ctDNA and hsDNA have relative weak RLS intensities, but strongly enhanced RLS signals with a maximum RLS peak at 402 nm appeared when AHs mixed with ctDNA or hsDNA. Another eight shoulder peaks can also be observed over the whole wavelength range of 250–600 nm. So the enhanced RLS signals resulting from the mixture of AHs and DNA indicated that an interaction has occurred between AHs and ctDNA or hsDNA (Yang *et al*., 2002). In addition, all of these enhanced RLS signals were enlarged regularly with increasing concentration of AHs. So the linear relationships between the mole concentrations of AHs and the RLS intensities of AHs-DNA were established (Table 2), for which the linearity coefficient are 0.9982 and 0.9947 for ctDNA and hsDNA, respectively.

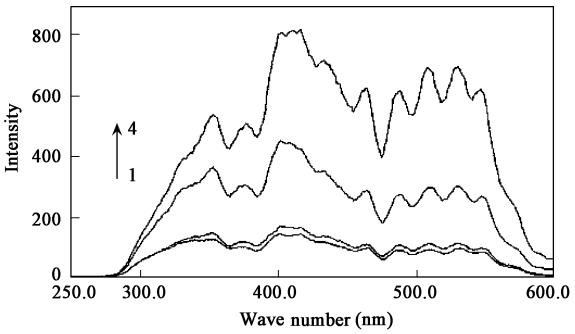

Fig. 6 RLS spectra of the interaction of ctDNA with AHs. (1) ctDNA (1.4×10^{-4} mol/L); (2) AHs (3.3×10^{-5} mol/L); (3) ctDNA (1.4×10^{-4} mol/L) + AHs (2.6×10^{-5} mol/L); (4) ctDNA (1.4×10^{-4} mol/L) + AHs (4.2×10^{-5} mol/L).

Table 2 Linear relationships between the total mole concentrations (C) of AHs and complex RLS intensities (I) of DNA with AHs

Nucleic acid name	Linear range of AHs concentrations ($\times10^{-6}$ mol/L)	Linear regression equation	Linearity coefficient (R)
ctDNA	3.3–100	I=33.84+1.0×10^7C	0.9982
hsDNA	3.3–85	I=45.01+2.0×10^7C	0.9947

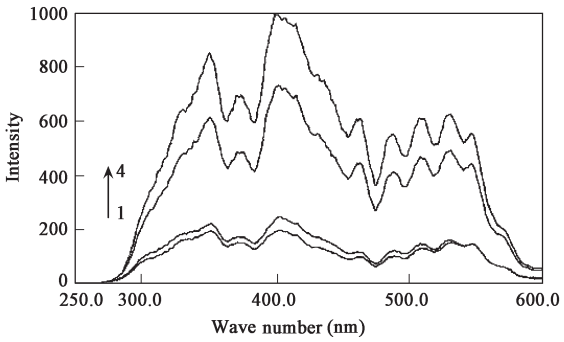

Fig. 7 RLS spectra of the interaction of hsDNA with AHs. (1) hsDNA (2.4×10^{-4} mol/L); (2) AHs (3.3×10^{-5} mol/L); (3): hsDNA (2.4×10^{-4} mol/L) + AHs (3.4×10^{-5} mol/L); (4) hsDNA (2.4×10^{-4} mol/L) + AHs (5.1×10^{-5} mol/L).

From the change of absorption and fluorescence spectra, we can deduce that the AHs fraction in the TSP can bind with ctDNA or hsDNA *in vitro*. That the fluorescence intensity of AHs fraction was quenched regularly by different concentration DNA indicated that some active components of AHs fraction may be intercalating the DNA bases. Further study about interaction mechanism did not performed due to the complicacy of component of AHs fraction in the TSP. The regularly change of RLS spectra in AHs, DNA and the mixture of AHs with DNA not only further supported that the binding occured between the AHs fraction and DNA but established the good linear relationships of dose-effect in the total contents of AHs with genotoxicity results.

3 Conclusions

The study results of this paper demonstrate that the AHs in atmospheric particulates of Xigu District of Lanzhou City, China, contain some active components, which direct react with DNA *in vitro* without any activation or metabolizing by organism. The results also indicated that the binding of AHs with hsDNA is stronger than that of with ctDNA. In addition, the good relationships of dose-effect between the total mole concentration of AHs and the ability of binding DNA were established by RLS spectroscopic method from chemical standpoint.

References

Aich P, Sen R, Dasgupta D, 1992. Role of magnesium ion in the interaction between chromomycin A3 and DNA: binding of chromomycin A3-Mg^{2+} complexes with DNA[J]. Biochemistry, 31: 2988–2997.

Ames B N, McCann J, Yamasaki E, 1975. Methods for detecting carcinogens and mutagens with the salmonella/mammalian-microsome mutagenicity test[J]. Mutat Res, 31: 347–363.

Bert B, Stephen T H, 2002. Air pollution and health[J]. Lancet, 360: 1233–1242.

Dockery D W, 2001. Epidemiologic evidence of cardiovascular effects of particulate air pollution[J]. Environ Health Perspect, 109(4): 483–486.

Guo D S, Yuan X Y, Zhang Z Q, 2000. Binding reaction of polycyclic aromatic hydrocarbons (PAHs) in floating dust of Taiyuan City with DNA[J]. China Environmental Science, 20: 5–7.

Gupta M, Ali R J B, 1984. Fluorescence studies on the interaction of furocoumarins with DNA in the dark[J]. Journal of Biochemistry, 95: 1253–1257.

Hiatt H H, Watson J D, Winsten J A, 1977. Origins of human cancer[M]. New York: Cold Spring Harbor Laboratory, Cold Spring Harbor.

Huang Y R, Ou Q Y, Yu W L, 1990. Characteristics of flame ionization detection for the quantitative analysis of complex organic mixtures[J]. Anal Chem, 62: 2063–2064.

Huang C Z, Li Y F, Fang P *et al*., 2001. Determination of proteins by their enhancement of resonance light scattering by fuchsine acid[J]. Fresenius J Anal Chem, 371: 1034–1036.

IARC Monographs, 1994. Cadmium and cadmium compounds[G]. Lyon.

IARC Monographs, 1990. Chromium, Nickel and Welding[G]. Vol.49, Lyon.

Kyrtopoulos S A, Anderson L M, Chhabra S K *et al*., 1997. DNA adducts and the mechanism of carcinogenesis and cytotoxicity of methylating agents of environmental and clinical significance[J]. Cancer Detect Prev, 21: 391–405.

Lakowica J R, 1999. Principles of fluorescence spectroscopy[M]. 2nd ed. New York: Kluwer/ Plenum.

Liu J Q, Tian J N, Zhang J Y *et al*., 2003. Interaction of magnolol with bovine serum albumin: a fluorescence quenching study[J]. Anal Bioanal Chem, 376: 864–867.

Martel L, Gagnon J, Masse R *et al*., 1986. Polycyclic aromatic hydrocarbons in sediments from the Saguenay Fjord, Canada[J]. Bull Environ Contam Toxicol, 37: 133–140.

Marzin D, 1999. New approaches to estimating the mutagenic potential of chemicals[J]. Cell Biology and Toxicology, 15: 359–365.

Pasternack R F, Collings P J, 1995. Resonance light scattering: a new technique for studying chromophore aggregation[J]. Science, 269: 935–939.

Plsavento M, Porfumo A, 1991. Interaction of serum albumin with a sulphonated azo dye in acidic solution[J]. Talanta, 38: 1099–1106.

Pope C A III, 1996. Adverse health effects of air pollutants in a nonsmoking population[J]. Toxicology, 111: 149–155.

Scatchard G, Scheiberg I I, Armstrong S H, 1950. Physical chemistry of protein solutions. IV. The combination of human serum albumin with chloride ion[J]. J Am Chem Soc, 72: 535–540.

Schwartz J, 2000. Harvesting and long-term exposure effects in the relation between air pollution and mortality[J]. Am J Epidemiol, 151: 440–448.

Sicre M A, Marty J C, Saliot A, 1987. Aliphatic and aromatic hydrocarbons in different sized aerosols over the Mediterranean sea: occurrence and origin[J]. Atmos Environ, 21: 2247–2259.

Sun Y Z, Zhang H J, Du Z C *et al*., 2003. Organic pollution of street dust in the Handan City, China[J]. Bull Environ Contam Toxicol, 70: 422–429.

Tian J N, Liu J Q, Zhang J Y *et al*., 2003. Fluorescence studies on the interactions of barbaloin with bovine serum[J]. Chem Pharm Bull, 51: 579–582.

Tysoe S A, Morgan R J, Baker A D *et al*., 1993. Spectroscopic investigation of differential binding modes of △- and ∧-$Ru(bpy)_2(ppz)^{2+}$ with calf thymus DNA[J]. J Phys Chem, 97: 1707–1711.

Wu H L, Li W Y, He X W *et al*., 2002. Spectral studies of the binding of lucigenin, a bisacridinium derivative, with double-helix DNA[J]. Anal Bioanal Chem, 373: 163–168.

Yang C X, Li Y F, Huang C Z, 2002. Determination of cationic surfactants in water samples by their enhanced resonance light scattering with azoviolet[J]. Anal Bioanal Chem, 374: 868–872.

You J, Lao W, Wang G, 1999. Analysis of organic pollutants in sewage by supercritical fluid extraction[J]. Chromatographia, 49: 399–405.

Zhang L, Chen C H, Li S X *et al*., 2000. Air pollution and potential control schemes in Lanzhou[J]. Res Environ Sci, 13: 18–21.

Zhang W J, Xu H P, Xue C X *et al*., 2001. Resonance light scattering for the determination of nucleic acids with methyl violet[J]. Anal Letter, 34: 553–568.